

# A Chemical Route to Activation of Open Metal Sites in the Copper-Based Metal–Organic Framework Materials HKUST-1 and Cu-MOF-2

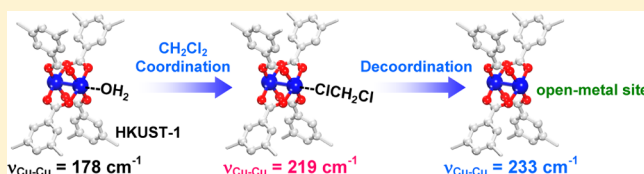
Hong Ki Kim,<sup>†</sup> Won Seok Yun,<sup>†</sup> Min-Bum Kim,<sup>‡</sup> Jeung Yoon Kim,<sup>†</sup> Youn-Sang Bae,<sup>‡</sup> JaeDong Lee,<sup>†</sup> and Nak Cheon Jeong<sup>\*,†</sup>

<sup>†</sup>Department of Emerging Materials Science, DGIST, Daegu 711-873, Korea

<sup>‡</sup>Department of Chemical and Biomolecular Engineering, Yonsei University, Seoul 120-749, Korea

## Supporting Information

**ABSTRACT:** Open coordination sites (OCSs) in metal–organic frameworks (MOFs) often function as key factors in the potential applications of MOFs, such as gas separation, gas sorption, and catalysis. For these applications, the activation process to remove the solvent molecules coordinated at the OCSs is an essential step that must be performed prior to use of the MOFs. To date, the thermal method performed by applying heat and vacuum has been the only method for such activation. In this report, we demonstrate that methylene chloride (MC) itself can perform the activation role: this process can serve as an alternative “chemical route” for the activation that does not require applying heat. To the best of our knowledge, no previous study has demonstrated this function of MC, although MC has been popularly used in the pretreatment step prior to the thermal activation process. On the basis of a Raman study, we propose a plausible mechanism for the chemical activation, in which the function of MC is possibly due to its coordination with the Cu<sup>2+</sup> center and subsequent spontaneous decooordination. Using HKUST-1 film, we further demonstrate that this chemical activation route is highly suitable for activating large-area MOF films.



## INTRODUCTION

Metal–organic frameworks (MOFs) are an intriguing class of nanoporous crystalline solids that are assembled by an alternating interconnection of inorganic nodes (either metal ions or metal oxide clusters) with multitopic organic linkers.<sup>1–7</sup> In many instances, open coordination sites (OCSs), coordinatively vacatable sites at the metal center (typically where Lewis base (LB) molecules can ligate with weak coordination bonding to be reversibly dissociable), have been demonstrated to play an important role in potential applications of MOFs, such as chemical separation,<sup>8–10</sup> gas storage,<sup>8,11–18</sup> heterogeneous catalysis,<sup>8,19–21</sup> sensing,<sup>22</sup> and ion conduction,<sup>8,23,24</sup> among others.<sup>25,26</sup>

HKUST-1, an MOF that is constructed of multiple links of paddle-wheel-like coordination between two Cu<sup>2+</sup> ions and four 1,3,5-benzenetricarboxylate (BTC) linkers (see Figure 1), is a good example of an MOF that possesses a very high concentration of OCSs.<sup>27</sup> A feature of HKUST-1 is that two types of large cages are three-dimensionally interconnected in an alternating fashion with a face-centered cubic topology (see the Supporting Information, Section S2). Another good example of an OCS-containing MOF is the MOF-2 series, which comprises transition metal ions such as Cu<sup>2+</sup> or Zn<sup>2+</sup> and 1,4-benzenedicarboxylate (BDC) linkers. The coordination mode in MOF-2 is same as the coordination mode in HKUST-1. However, in contrast to HKUST-1, the architecture of MOF-2 is based on stacking lamellar phase sheets of Cu<sub>2</sub>(BDC)<sub>2</sub> in two dimensions. The “extracoordination” (solvent coordination) ability of the OCSs in both HKUST-1

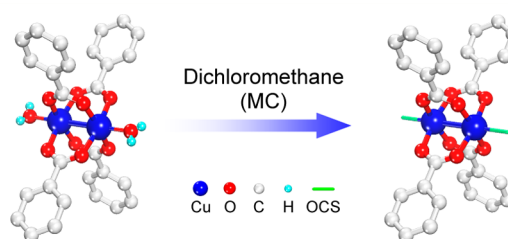


**Figure 1.** Schematic illustration of chemical activation of the paddle-wheel-like (Cu<sup>II</sup>)<sub>2</sub> node within HKUST-1 or Cu-MOF-2 performed by MC. Hydrogen atoms bound to carbon atoms in the benzene moieties are omitted for the sake of clarity.

and MOF-2 enables them to be excellent adsorbents or molecule separators for applications such as carbon dioxide sorption,<sup>11,28,29</sup> water sorption,<sup>30</sup> amine sorption,<sup>31</sup> nitric oxide capture,<sup>32</sup> water/ethanol separation,<sup>33</sup> and others.<sup>9,19,20,22–24,34–36</sup>

To utilize that type of MOF for the aforementioned applications, an activation process to remove both pre-coordinating solvent molecules from the OCS and pore-filling guest molecules (typically the solvents used during the synthesis process) from the pores is a prerequisite step.<sup>37</sup> To date, five strategies<sup>38</sup> for effective activation have been developed: (i) thermal activation (by applying heat and vacuum; hereafter

Received: June 30, 2015

Published: July 21, 2015

TA),<sup>39–43</sup> (ii) solvent exchange (typically performed by methylene chloride or chloroform),<sup>44,45</sup> (iii) freeze-drying,<sup>46</sup> (iv) supercritical CO<sub>2</sub> exchange,<sup>45</sup> and (v) chemical treatment (typically with HCl only in the cases where corresponding MOFs are exceptionally stable in strong acidic environment, for examples, MOFs constructed with zirconium oxide cluster such as PCN-222 (also known as MOF-545) and NU-1000).<sup>21,25,47</sup> Among these strategies, TA has been most commonly used because it can completely remove pore-filling solvents and it is the only known method that can remove components of both coordinated and pore-filling solvents. However, often characterized by TA's negative influence on structural integrity,<sup>37,45,48,49</sup> the TA process has evolved by combining it with the solvent exchange method because employment of a solvent with a lower boiling point, e.g., methylene chloride (CH<sub>2</sub>Cl<sub>2</sub>, hereafter MC) or chloroform (CHCl<sub>3</sub>), can aid in lowering the activation temperature and thereby minimizing the potential structural damage. Yaghi and co-workers first demonstrated that treatment with chloroform prior to TA is quite effective for complete removal of the pore-filling solvent under mild conditions.<sup>44</sup> However, it is surprising that although such solvents (e.g., CH<sub>2</sub>Cl<sub>2</sub> or CHCl<sub>3</sub>) have frequently been used in solvent exchange processes to support permanent porosity by removing pore-filling solvents, to the best of our knowledge, there has been no systematic study of their secondary function, i.e., scissoring the solvent coordination at the OCS. Here, we report regarding the scissoring function of MC. Although several MOFs that possess OCSs should be suitable for this demonstration, we limited our studies to HKUST-1 and Cu-MOF-2. As described below, we found that soaking HKUST-1 or MOF-2 in fresh MC for only 5 min at room temperature and subsequent repetition of the process several times led to decoordination of the H<sub>2</sub>O, EtOH, MeOH, MeCN, and even dimethylformamide (DMF) bound to the OCSs (see Figure 1). Also, we suggest a plausible mechanism for this “chemical activation” route on the basis of Raman studies. Furthermore, we demonstrate that this chemical activation process is highly useful for activating large-area films, which is likely to be costly and cumbersome due to the requirement of massive equipment for applying heat and vacuum when the conventional thermal method is used for the activation.<sup>37</sup>

## RESULTS AND DISCUSSION

HKUST-1 contains two types of large cages (type 1 and type 2 cages), a type of corner-sharing small cage (a type 3 cage), and two types of windows (see the Section S2 of the Supporting Information for details). Regarding its structure, alternative face centered cubic (fcc) close packing of the type 1 and type 2 cages constructs HKUST-1. Whereas the small cages (type 3) formed at the edges of the large cages preclude free access of guest molecules because of aperture blockage by the benzene moiety in BTC, the large cages allow fast access to guests through their large open spaces. What is notable is that all OCSs face toward the open spaces of the large cages (type 1). This fact thus makes HKUST-1 more valuable because guest molecules can be more readily accessible to the OCS, and the molecules decoordinated from the OCS can be readily removed through the large open spaces. In addition, HKUST-1 has the ability to replace its pre-coordinated solvent with other Lewis base polar guest molecules when the Lewis base molecules are sufficiently fed.<sup>23,37</sup> With this fact in mind, we questioned whether even MC can be substituted by exchanging the

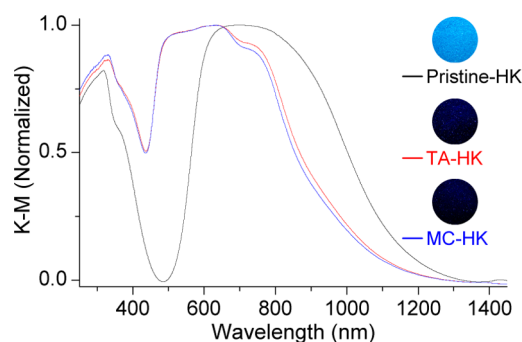


**Figure 2.** Diffuse reflectance UV-vis absorption spectra of pristine-HK (black curve), TA-HK (red curve), and MC-HK (blue curve) crystalline powders. The circular insets show optical microscope images of the samples as indicated.

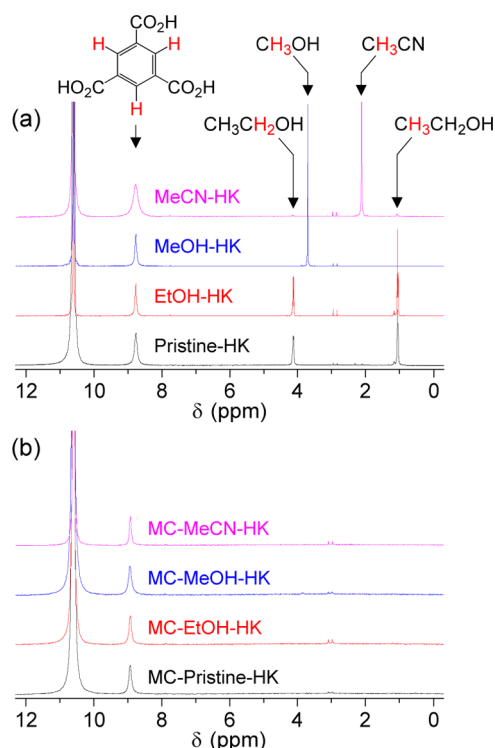


**Figure 3.** <sup>1</sup>H NMR spectra of pristine-, EtOH-, MeOH-, and MeCN-coordinated HKUST-1 (a) before and (b) after MC treatment. The NMR spectra were taken after completely dissolving the powder samples in D<sub>2</sub>SO<sub>4</sub>.

pre-coordinated H<sub>2</sub>O and EtOH (solvents used in synthesis) in pristine HKUST-1, although the polarity of MC is much less, considering the primitive assumption that the MC is also a weak Lewis base that possesses lone-paired electrons in its chlorine atoms.<sup>50–54</sup> Our postulate was that if the MC molecules can be replaced, the coordination of MC will be substantially more than sufficiently labile to be spontaneously dissociated with a low activation energy (thermal energy at room temperature). If it is so labile, then MC treatment itself in the absence of supplied heat can be an effective, cost-effective chemical method for activation of OCSs.

Our first step to address the question was to observe the color change of HKUST-1 after MC treatment without applying heat, assuming that the color change would be significantly influenced by coordination around the Cu<sup>2+</sup>

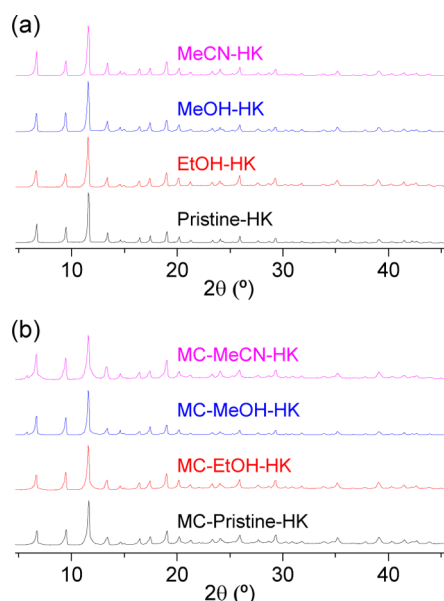


**Figure 4.** PXRD patterns of pristine-, EtOH-, MeOH-, and MeCN-coordinated HKUST-1 (a) before and (b) after MC treatment.

centers. We observed that whereas pristine HKUST-1 is sky blue, its color turned to deep navy blue after MC treatment (see the optical microscope image and ultraviolet–visible (UV–vis) absorption spectra shown in Figure 2). Also notable is that the pattern of the color change after the MC treatment was exactly the same as the pattern after TA which has been a unique method to completely remove all of the ligated solvents (see Figure 2). The UV–vis absorption of pristine HKUST-1 originates from ligand-to-metal charge transfer (LMCT) and d–d transitions around the  $\text{Cu}^{2+}$  centers.<sup>55</sup> The absorption band at energies greater than 2.5 eV (less than approximately 500 nm in wavelength) is due to the LMCT from oxygen in the carboxylate to  $\text{Cu}^{2+}$  ions, and the absorption band at energies less than 2.5 eV (greater than approximately 500 nm in wavelength) is due to the d–d transition around the  $\text{Cu}^{2+}$  centers.<sup>55</sup> The aforementioned color changes are due to the shift of the d–d transition, which, in principle, reflects the changes in the chemical environment around the  $\text{Cu}^{2+}$  centers (ligand coordination or coordination-free state). More precisely, we speculate that the blue shift is a result of a partial decrease in the number of electrons surrounding  $\text{Cu}^{2+}$  ion and a loss of degeneracy in d-orbital level arisen by changes in the number of ligand and the geometry around  $\text{Cu}^{2+}$  center after loss of  $\text{H}_2\text{O}$  and EtOH coordination.<sup>55,56</sup> Given that both the TA and MC treatments led to the same extent of blue shift in their absorption spectra, we tentatively speculate that MC itself can function as a reagent for chemical activation of  $\text{Cu}^{2+}$  centers, thereby forming an intermediate state of MC coordination (more information about this intermediate state is provided in the discussion of our Raman study presented below).

To provide concrete evidence for the chemical activation behavior of MC, we employed  $^1\text{H}$ -nuclear magnetic resonance (NMR) spectroscopic analysis. For systematic analyses, we prepared pure EtOH-, MeOH-, and MeCN-coordinated HKUST-1 (EtOH-HK, MeOH-HK, and MeCN-HK, respectively; HK = fully desolvated HKUST-1) and MC-treated EtOH-HK, MeOH-HK, and MeCN-HK (MC-EtOH-HK, MC-MeOH-HK, and MC-MeCN-HK, respectively). Thermally

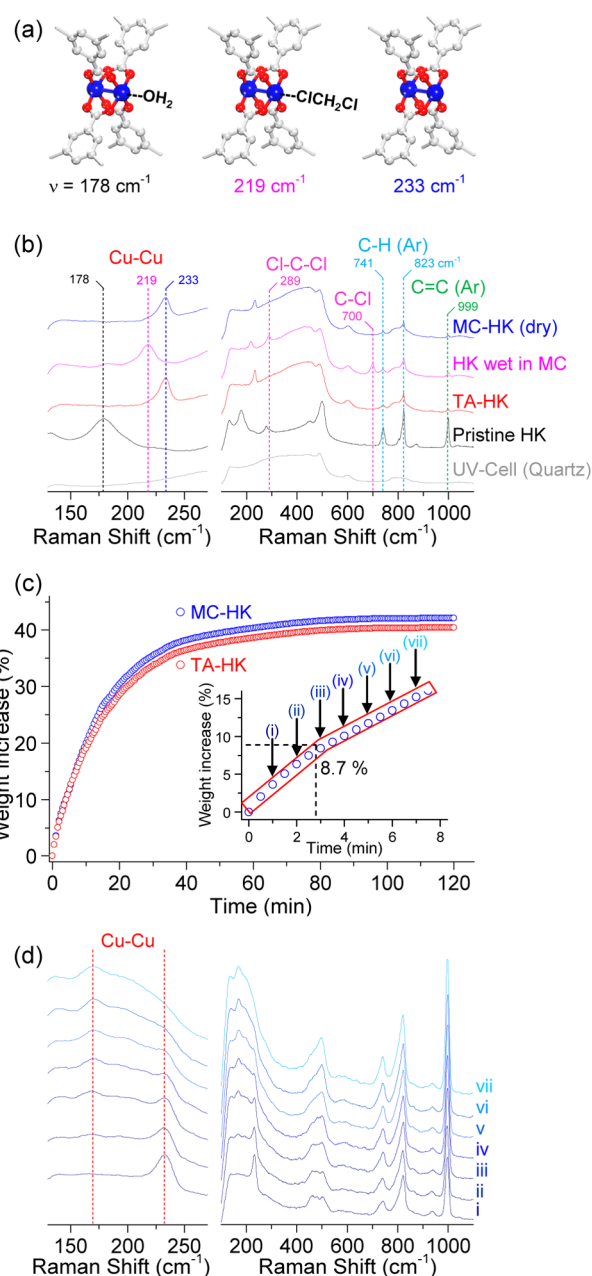


**Figure 5.** (a) Illustration of  $\text{H}_2\text{O}$ -coordinated,  $\text{CH}_2\text{Cl}_2$ -coordinated, and ligand-free ( $\text{Cu}^{\text{II}}_2$ ) centers. (b) Expanded (left panel) and wide (right panel) views of Raman spectra obtained from bare quartz container (gray curve), pristine-HK (black curve), TA-HK (red curve), HK wet in MC (pink curve), and dry MC-HK (blue curve) samples. (c) Plots of increase in the weights of the TA-HK and MC-HK samples with respect to the exposure time to ambient atmosphere (approximately 30% relative humidity). The inset shows the weight change of the MC-HK sample in the initial exposure. (d) Expanded (left panel) and wide (right panel) views of the spectral changes in the Raman shifts of a dry MC-HK sample according to the exposure time to ambient atmosphere in intervals of 3 min [i.e., after (i) 0, (ii) 3, (iii) 6, (iv) 9, (v) 12, (vi) 15, and (vii) 18 min].

activated HKUST-1 (TA-HK) was also prepared for comparison. Both the  $\text{H}_2\text{O}$  and EtOH in pristine-HK were preferentially removed via TA at 150 °C for 12 h under vacuum. The TA-HK samples were then placed in a moisture-free Ar-charged glovebox and allowed to coordinate with pure EtOH, MeOH, or MeCN by soaking in the corresponding neat



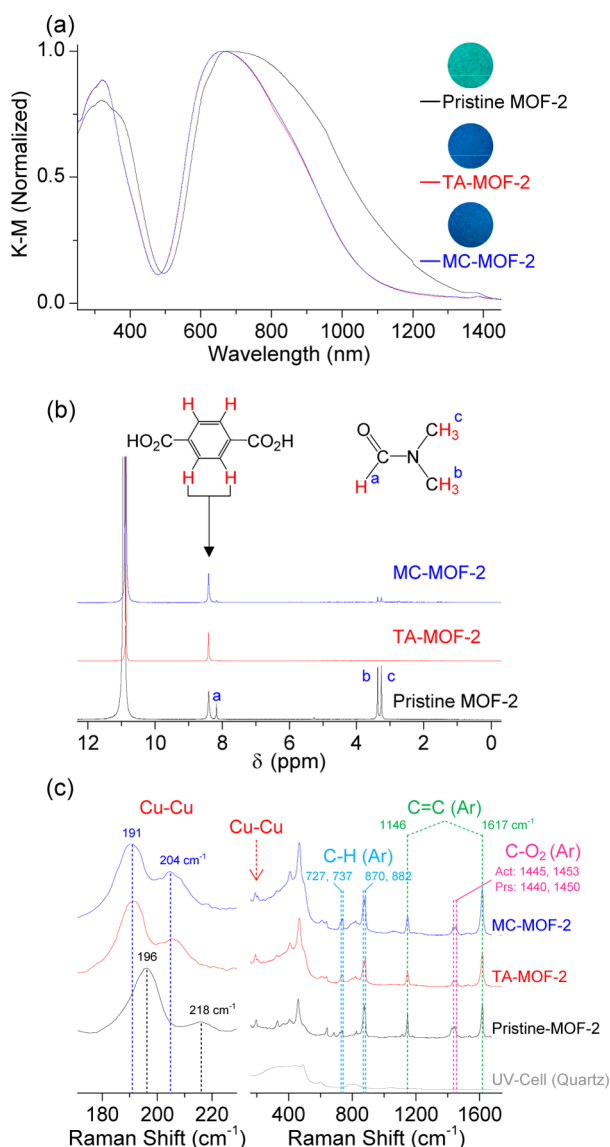


**Figure 6.** (a) Diffuse reflectance UV–vis absorption spectra of pristine-MOF-2 (black curve), TA-MOF-2 (red curve), and MC-MOF-2 (blue curve) crystalline powders. The optical microscope images in the circular insets display the colors of the powder samples. (b) <sup>1</sup>H NMR spectra of pristine-MOF-2, TA-MOF-2, and MC-MOF-2 taken after the samples were dissolved in D<sub>2</sub>SO<sub>4</sub>. (c) Expanded (left panel) and wide (right panel) views of the Raman spectra of pristine-, TA-, and MC-MOF-2 powder samples. The Raman spectra were taken after the samples were sealed in a moisture-free argon-charged glovebox.

solvent to prepare EtOH-HK, MeOH-HK, and MeCN-HK (see Section S1 of the Supporting Information for details). MC treatment of pristine-HK, EtOH-HK, MeOH-HK, and MeCN-HK was performed by soaking the corresponding powder sample in pure MC solvent at room temperature for 5 min, and this procedure was repeated 5 times to ensure the completeness of the treatment. Figure 3 shows <sup>1</sup>H NMR spectra of pristine-HK, EtOH-HK, MeOH-HK, MeCN-HK, MC-pristine-HK, MC-EtOH-HK, MC-MeOH-HK, and MC-MeCN-HK. The spectra were taken after each powder sample was dissolved in deuterated sulfuric acid, D<sub>2</sub>SO<sub>4</sub>.<sup>23</sup> Whereas the peak for the three identical protons in BTC appears at 8.8 ppm, peaks for the two identical CH<sub>2</sub> protons and three identical CH<sub>3</sub> protons

in EtOH appear at 4.1 and 1.1 ppm, respectively. In addition, the peaks for the three identical CH<sub>3</sub> protons in MeOH and MeCN appear at 3.7 and 2.1 ppm, respectively. The peak for the protons in water and the hydroxyl group in alcohols appears at ~10.6 ppm because the proton forms hydronium ion (H<sub>3</sub>O<sup>+</sup>) by combining with sulfuric acid. As expected, the peaks for EtOH in pristine-HK disappeared after TA was performed (see the <sup>1</sup>H NMR spectrum presented in Section S3 of the Supporting Information). It is also interesting that the spectrum of MC-pristine-HK is identical to the spectrum of TA-HK. We observed that this behavior was generic for all of the MC-EtOH-HK, MC-MeOH-HK, and MC-MeCN-HK samples (see Figure 3b). These results thus underscore the ability of MC to perform chemical activation of OCSs.

The phase purities of pristine-HK, EtOH-HK, MeOH-HK, and MeCN-HK before and after MC treatment were determined via powder X-ray diffraction (PXRD) measurements (see Figure 4). The PXRD patterns of MC-treated samples indicated that the structural integrity of the MOF was well preserved even though the solvent coordination was removed. To confirm this structural integrity, we also tested N<sub>2</sub> isotherms (BET) of both pristine-HK and MC-pristine-HK. Whereas the pristine-HK was treated by TA at 150 °C under vacuum before the BET measurement, the MC-pristine-HK sample was pretreated only by applying vacuum at room temperature (see Sections S1 and S4 of the Supporting Information for details). The resulting internal surface area of the samples (approximately 1740 m<sup>2</sup>·g<sup>-1</sup> for TA-Pristine-HK and approximately 1690 m<sup>2</sup>·g<sup>-1</sup> for MC-Pristine-HK) were consistent within the (acceptable) error range (see Section S4 of the Supporting Information for details). Thus, these PXRD and BET results provide compelling evidence for the safety of MC treatment in terms of structural integrity.

We hypothesized that the change in coordination around the Cu<sup>2+</sup> centers (presence or absence of the extracoordination of solvents) would be reflected in the vibrational strength of the Cu–Cu bonding. To test this hypothesis, we monitored Raman spectra of pristine-HK before and after MC treatment. A TA-pristine-HK sample was also examined for comparison. To avoid exposure to a moist atmosphere, we prepared the Raman samples by sealing them in disc-shaped quartz containers under the moisture-free conditions of an Ar-charged glovebox. Whereas the stretching vibration mode of Cu–Cu bonding in the pristine-HK appeared at the shift of approximately 178 cm<sup>-1</sup>, the stretching vibrations in both MC-pristine-HK and TA-pristine-HK samples appeared at similar shifts of approximately 233 cm<sup>-1</sup> (see Figure 5a and 5b).<sup>55</sup> (We note that the peak that appeared at 289 cm<sup>-1</sup> was due to the scissoring vibration mode of Cl–C–Cl in MC. See Section S5 of the Supporting Information for details.) The experimental values of 178 and 233 cm<sup>-1</sup> agree well with the values theoretically calculated for the vibration mode of H<sub>2</sub>O-coordinated (211 cm<sup>-1</sup>) and open-state (233 cm<sup>-1</sup>) Cu–Cu centers, respectively (see Supporting Information, Section S6). This seemingly similar trend is highly consistent with the trend in the above NMR results. Nevertheless, it was interesting that in terms of the Raman shift, a pristine-HK sample wet in pure MC solvent was strikingly different from a dry version of the sample. The Raman shift of MC-wet HKUST-1 appeared at approximately 219 cm<sup>-1</sup> (see Figure 5a and 5b), thus demonstrating the presence of MC-coordination as an intermediate state. This observation reasonably supports our primary postulate: coordination and decoordination of MC

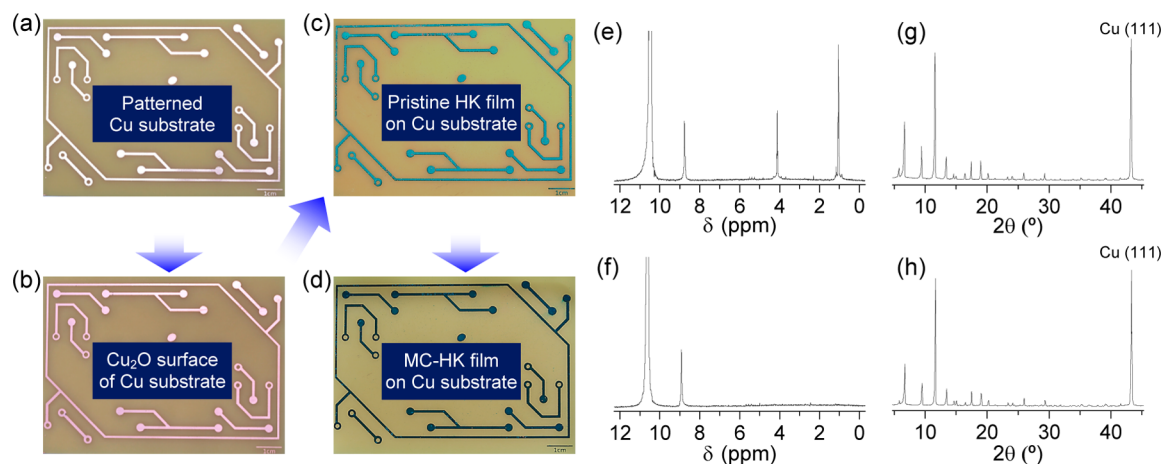


**Figure 7.** Photographs of the (a) patterned Cu substrate, (b) surface-oxidized Cu substrate ( $\text{Cu}_2\text{O}/\text{Cu}$ ), (c) pristine HKUST-1 film synthesized on the Cu substrate, and (d) MC-treated HKUST-1 film.  $^1\text{H}$  NMR spectra of (e) pristine- and (f) MC-treated HKUST-1 films. XRD patterns of (g) pristine- and (h) MC-treated HKUST-1 films.

during the MC treatment process (see above). That is, a sequential two-step reaction—coordination of MC through the Cl-bridge formed after replacement of the pre-coordinated solvents and subsequent spontaneous decoordination of MC—is a plausible mechanism for the chemical activation process (see Section S6 of Supporting Information).<sup>50–54</sup> Using Badger's rule, we could also estimate that the bond strength of the Cu–Cu bonding decreases in the following order: activated-HK > MC-coordinated-HK > pristine-HK.

Another clue regarding the chemical activation is the presence/absence of the open-state of the OCSs that are formed after MC treatment. The presence of the open-state can be checked by monitoring the coordination of moist  $\text{H}_2\text{O}$  molecules in an activated sample. We examined the weight increase of the MC-treated HKUST-1 sample after exposing to moist air (relative humidity = ca. 30%). The test showed an instantaneous increase in weight by  $\sim 42\%$  (see Figure 5c). Here, we noted an inflection point appearing at  $\sim 8.7\%$  because this value is very close to the value (8.9%) theoretically calculated for the maximum amount of  $\text{H}_2\text{O}$  coordinating at the OCSs. (We assumed that weight increase by the coordination of  $\text{O}_2$ ,  $\text{N}_2$ ,  $\text{CO}$ ,  $\text{CO}_2$ , and other gases in ambient air is likely to be negligible.) Thus, the inflection point indicates that most OCSs in the MC-treated sample remains in the open-state after the chemical activation. We attribute the further increase over 8.7% to the pore filling of moist water. A similar pattern of weight increase was observed for the TA-HK sample (see Figure 5c). Furthermore, coordination of moist  $\text{H}_2\text{O}$  was directly observed via Raman spectroscopy. Whereas the initial peak at  $233\text{ cm}^{-1}$  (open-state) gradually decreased, the peak at  $178\text{ cm}^{-1}$  ( $\text{H}_2\text{O}$ -coordinated) gradually increased as the exposure time to ambient air increased (see Figure 5d and Section S7 of the Supporting Information). Also notable is that the peaks were ratiometric at independent positions rather than continuously shifting from  $233$  to  $178\text{ cm}^{-1}$ . This thereby demonstrates that although all  $\text{Cu}^{2+}$  centers in HKUST-1 are interconnected through BTC ligands, the Cu–Cu vibrations are not interactive.

We also tested Cu-MOF-2 to address whether the chemical activation behavior of MC could be expanded. Crystalline Cu-MOF-2 powder was synthesized from the sources of  $\text{Cu}(\text{NO}_3)_2$  and BDC using DMF solvent (the experimental details are presented in Section S1 of the Supporting Information). We

observed that the color of Cu-MOF-2 changed from light green to dark blue after the sample was thermally activated. The MC treatment also exhibited a similar color change, thus implying its activation function even in Cu-MOF-2 (see Figure 6a). UV–vis absorption spectra of the MOF-2 samples clearly indicate that the color change is caused by the blue-shift of the d–d transition, similar to the pattern observed in HKUST-1.<sup>55</sup> To further understand this behavior, we examined  $^1\text{H}$  NMR analysis. The  $^1\text{H}$  NMR spectrum of pristine MOF-2 powder shows that it contains DMF as a coordinating component at the OCSs (see Figure 6b). Consistent with the above result, the coordinated DMF was dissociated after MC treatment (the experimental details are presented in Section S1 of the Supporting Information). Meanwhile, the phase of MOF-2 was transformed after the TA process, as previously reported in literature (see Section S8 of the Supporting Information).<sup>57,58</sup> The chemical activation also resulted in PXRD patterns quite similar to those of the TA, indicating that its 2-dimensional framework was not collapsed after the chemical activation. In terms of the Raman spectra, MOF-2 exhibited behavior that differed from that of HKUST-1 in two aspects (see Figure 6c). One aspect is that the Raman shift involving the Cu–Cu stretching vibration appeared as a doublet mode at  $196$  and  $218\text{ cm}^{-1}$ . The other aspect is that whereas HKUST-1 exhibited a blue-shift in the Cu–Cu vibration after activation (from  $178$  to  $233\text{ cm}^{-1}$ ), MOF-2 exhibited red-shifts in both peaks of the doublet (from  $196$  to  $191\text{ cm}^{-1}$  and from  $218$  to  $204\text{ cm}^{-1}$ ). Although more comprehensive studies are required to fully understand this behavior, our observation is in good agreement with the pattern reported in the literature.<sup>58</sup> Regardless, an important fact is that the pattern of the shift after chemical activation is exactly same as the pattern of the shift after TA. This evidence strongly supports our demonstration of the chemical activation behavior of MC in Cu-MOF-2.

TA, which is typically conducted by applying heat and vacuum, requires effective facilities to make the temperature of the surroundings higher and the pressure lower, at least relative to the atmospheric conditions. In contrast with TA, chemical activation is likely to be more useful when the amount of the powder sample or the size of the MOF films is large because such facilities are not required for this method. To test the feasibility of the MC treatment, we synthesized HKUST-1 film on metallic Cu substrate via an oxidation reaction (see Figure

7a, 7b, and 7c).<sup>59</sup> Whereas the color of the as-synthesized HKUST-1 film was sky blue, its color changed to dark blue after the MC treatment (see Figure 7d). In agreement with the results obtained from powder samples, the chemical activation process could completely remove the coordinated EtOH from the film (Figure 7e and 7f) and simultaneously preserve its framework well (Figure 7g and 7h).

## CONCLUSIONS

In summary, we have observed a “chemical activation” function of MC to remove the solvent coordination from OCSs of metal nodes. For the examples examined, the function of MC was clearly demonstrated not only by monitoring the dissolution of the <sup>1</sup>H NMR peaks for the solvent molecules coordinated at the OCSs but also by observing the Raman shift of the Cu–Cu vibration. In particular, the Raman studies enabled us to observe the presence of MC coordination as a conceivable intermediate state during the chemical activation reaction. We also confirmed that this chemical activation behavior does not appear if MC treatment is omitted in the process (for instance, when only vacuum is applied at room temperature for 2 h; see Section S9 of Supporting Information). Using HKUST-1 films synthesized on patterned copper plates, we have also demonstrated that this chemical method will be more useful for activating large-area MOF films as a cheap and facile process. We anticipate that this secondary role of MC will also be useful for the MOF industry, and the resulting guidelines will prove transferrable/adaptable to other MOFs that contains ligand-accessible metal ions, such as Zn-HKUST-1, MIL-101 and MOF-74.

## ASSOCIATED CONTENT

### Supporting Information

Experimental details, theoretical study, and PXRD, <sup>1</sup>H NMR, BET, and Raman data. The Supporting Information is available free of charge on the ACS Publications website at DOI: 10.1021/jacs.5b06637.

## AUTHOR INFORMATION

### Corresponding Author

\*nc@dgist.ac.kr

### Notes

The authors declare no competing financial interest.

## ACKNOWLEDGMENTS

This work was supported by the Ministry of Science, ICT, and Future Planning (MSIP) of Korea under the auspices of the Basic Science Research Program sponsored by the National Research Foundation (NRF) (Grant No. NRF-2013R1A1A1010254) and by the DGIST R&D Program (Grant No. 15-BD-0403). J.D. Lee also gratefully acknowledges support from MSIP of Korea under the auspices of the Basic Science Research Program sponsored by the NRF (Grant No. NRF-2013R1A1A2007388).

## REFERENCES

- (1) Yaghi, O. M.; Li, H.; Davis, C.; Richardson, D.; Groy, T. L. *Acc. Chem. Res.* **1998**, *31*, 474–484.
- (2) O’Keeffe, M.; Yaghi, O. M. *Chem. Rev.* **2012**, *112*, 675–702.
- (3) Zhou, H.-C.; Long, J. R.; Yaghi, O. M. *Chem. Rev.* **2012**, *112*, 673–674.
- (4) Li, M.; Li, D.; O’Keeffe, M.; Yaghi, O. M. *Chem. Rev.* **2014**, *114*, 1343–1370.

- (5) Deria, P.; Mondloch, J. E.; Karagiari, O.; Bury, W.; Hupp, J. T.; Farha, O. K. *Chem. Soc. Rev.* **2014**, *43*, 5896–5912.
- (6) Zhou, H.-C.; Kitagawa, S. *Chem. Soc. Rev.* **2014**, *43*, 5415–5418.
- (7) Gassensmith, J. J.; Kim, J. Y.; Holcroft, J. M.; Farha, O. K.; Stoddart, J. F.; Hupp, J. T.; Jeong, N. C. *J. Am. Chem. Soc.* **2014**, *136*, 8277–8282.
- (8) Furukawa, H.; Cordova, K. E.; O’Keeffe, M.; Yaghi, O. M. *Science* **2013**, *341*, 974.
- (9) Banerjee, D.; Cairns, A. J.; Liu, J.; Motkuri, R. K.; Nune, S. K.; Fernandez, C. A.; Krishna, R.; Strachan, D. M.; Thallapally, P. K. *Acc. Chem. Res.* **2015**, *48*, 211–219.
- (10) Bae, Y.-S.; Lee, C. Y.; Kim, K. C.; Farha, O. K.; Nickias, P.; Hupp, J. T.; Nguyen, S. T.; Snurr, R. Q. *Angew. Chem., Int. Ed.* **2012**, *51*, 1857–1860.
- (11) D’Alessandro, D. M.; Smit, B.; Long, J. R. *Angew. Chem., Int. Ed.* **2010**, *49*, 6058–6082.
- (12) Bae, Y.-S.; Snurr, R. Q. *Angew. Chem., Int. Ed.* **2011**, *50*, 11586–11596.
- (13) Lin, L.-C.; Kim, J.; Kong, X.; Scott, E.; McDonald, T. M.; Long, J. R.; Reimer, J. A.; Smit, B. *Angew. Chem., Int. Ed.* **2013**, *52*, 4410–4413.
- (14) Dinca, M.; Long, J. R. *Angew. Chem., Int. Ed.* **2008**, *47*, 6766–6779.
- (15) Eddaoudi, M.; Kim, J.; Rosi, N.; Vodak, D.; Wachter, J.; O’Keeffe, M.; Yaghi, O. M. *Science* **2002**, *295*, 469–472.
- (16) Peng, Y.; Krungleviciute, V.; Eryazici, I.; Hupp, J. T.; Farha, O. K.; Yildirim, T. *J. Am. Chem. Soc.* **2013**, *135*, 11887–11894.
- (17) He, Y.; Zhou, W.; Qian, G.; Chen, B. *Chem. Soc. Rev.* **2014**, *43*, 5657–5678.
- (18) Xiang, S.; Zhou, W.; Zhang, Z.; Green, M. A.; Liu, Y.; Chen, B. *Angew. Chem., Int. Ed.* **2010**, *49*, 4615–4618.
- (19) Lee, J.; Farha, O. K.; Roberts, J.; Scheidt, K. A.; Nguyen, S. T.; Hupp, J. T. *Chem. Soc. Rev.* **2009**, *38*, 1450–1459.
- (20) Schlichte, K.; Kratzke, T.; Kaskel, S. *Microporous Mesoporous Mater.* **2004**, *73*, 81–88.
- (21) Feng, D.; Gu, Z.-Y.; Li, J.-R.; Jiang, H.-L.; Wei, Z.; Zhou, H.-C. *Angew. Chem., Int. Ed.* **2012**, *51*, 10307–10310.
- (22) Kreno, L. E.; Leong, K.; Farha, O. K.; Allendorf, M.; Van Duyne, R. P.; Hupp, J. T. *Chem. Rev.* **2012**, *112*, 1105–1125.
- (23) Jeong, N. C.; Samanta, B.; Lee, C. Y.; Farha, O. K.; Hupp, J. T. *J. Am. Chem. Soc.* **2012**, *134*, 51–54.
- (24) Ramaswamy, P.; Wong, N. E.; Shimizu, G. K. H. *Chem. Soc. Rev.* **2014**, *43*, 5913–5932.
- (25) Mondloch, J. E.; Bury, W.; Fairen-Jimenez, D.; Kwon, S.; DeMarco, E. J.; Weston, M. H.; Sarjeant, A. A.; Nguyen, S. T.; Stair, P. C.; Snurr, R. Q.; Farha, O. K.; Hupp, J. T. *J. Am. Chem. Soc.* **2013**, *135*, 10294–10297.
- (26) Barea, E.; Montoro, C.; Navarro, J. A. R. *Chem. Soc. Rev.* **2014**, *43*, 5419–5430.
- (27) Chui, S. S.-Y.; Lo, S. M.-F.; Charmant, J. P. H.; Orpen, A. G.; Williams, I. D. *Science* **1999**, *283*, 1148–1150.
- (28) Eddaoudi, M.; Li, H.; Yaghi, O. M. *J. Am. Chem. Soc.* **2000**, *122*, 1391–1397.
- (29) Yazaydin, A. O.; Benin, A. I.; Faheem, S. A.; Jakubczak, P.; Low, J. J.; Willis, R. R.; Snurr, R. Q. *Chem. Mater.* **2009**, *21*, 1425–1430.
- (30) Canivet, J.; Fateeva, A.; Guo, Y.; Coasne, B.; Farrusseng, D. *Chem. Soc. Rev.* **2014**, *43*, 5594–5617.
- (31) Borfecchia, E.; Maurelli, S.; Gianolio, D.; Groppo, E.; Chiesa, M.; Bonino, F.; Lamberti, C. *J. Phys. Chem. C* **2012**, *116*, 19839–19850.
- (32) Xiao, B.; Wheatley, P. S.; Zhao, X.; Fletcher, A. J.; Fox, S.; Rossi, A. G.; Megson, I. L.; Bordiga, S.; Regli, L.; Thomas, K. M.; Morris, R. E. *J. Am. Chem. Soc.* **2007**, *129*, 1203–1209.
- (33) de Lima, G. F.; Mavrandonakis, A.; de Abreu, H. A.; Duarte, H. A.; Heine, T. *J. Phys. Chem. C* **2013**, *117*, 4124–4130.
- (34) Munch, A. S.; Mertens, F. O. R. L. *J. Mater. Chem.* **2012**, *22*, 10228–10234.
- (35) Supronowicz, B.; Mavrandonakis, A.; Heine, T. *J. Phys. Chem. C* **2013**, *117*, 14570–14578.



- (36) Supronowicz, B.; Mavrandonakis, A.; Heine, T. *J. Phys. Chem. C* **2015**, *119*, 3024–3032.
- (37) Yang, Y.; Shukla, P.; Wang, S.; Rudolph, V.; Chen, X.-M.; Zhu, Z. *RSC Adv.* **2013**, *3*, 17065–17072.
- (38) Mondloch, J. E.; Karagiari, O.; Farha, O. K.; Hupp, J. T. *CrystEngComm* **2013**, *15*, 9258–9264.
- (39) Abrahams, B. F.; Hoskins, B. F.; Michail, D. M.; Robson, R. *Nature* **1994**, *369*, 727–729.
- (40) Li, H.; Eddaoudi, M.; Groy, T. L.; Yaghi, O. M. *J. Am. Chem. Soc.* **1998**, *120*, 8571–8572.
- (41) Kepert, C. J.; Rosseinsky, M. J. *Chem. Commun.* **1999**, 375–376.
- (42) Ferey, G.; Mellot-Draznieks, C.; Serre, C.; Millange, F.; Dutour, J.; Surble, S.; Margiolaki, I. *Science* **2005**, *309*, 2040–2042.
- (43) Cavka, J. H.; Jakobsen, S.; Olsbye, U.; Guillou, N.; Lamberti, C.; Bordiga, S.; Lillerud, K. P. *J. Am. Chem. Soc.* **2008**, *130*, 13850–13851.
- (44) Li, H.; Eddaoudi, M.; O’Keeffe, M.; Yaghi, O. M. *Nature* **1999**, *402*, 276–279.
- (45) Nelson, A. P.; Farha, O. K.; Mulfort, K. L.; Hupp, J. T. *J. Am. Chem. Soc.* **2009**, *131*, 458–460.
- (46) Lohe, M. R.; Rose, M.; Kaskel, S. *Chem. Commun.* **2009**, 6056–6058.
- (47) Morris, W.; Voloskiy, B.; Demir, S.; Gandara, F.; McGrier, P. L.; Furukawa, H.; Cascio, D.; Stoddart, J. F.; Yaghi, O. M. *Inorg. Chem.* **2012**, *51*, 6443–6445.
- (48) Tsao, C.-S.; Chen, C.-Y.; Chung, T.-Y.; Su, C.-J.; Su, C.-H.; Chen, H.-L.; Jeng, U.-S.; Yu, M.-S.; Liao, P.-Y.; Lin, K.-F.; Tzeng, Y.-R. *J. Phys. Chem. C* **2010**, *114*, 7014–7020.
- (49) Bhunia, M. K.; Hughes, J. T.; Fetting, J. C.; Navrotsky, A. *Langmuir* **2013**, *29*, 8140–8145.
- (50) Colman, M. R.; Noirot, M. D.; Miller, M. M.; Anderson, O. P.; Strauss, S. H. *J. Am. Chem. Soc.* **1988**, *110*, 6886–6888.
- (51) Newbound, T. D.; Colman, M. R.; Miller, M. M.; Wulfsberg, G. P.; Anderson, O. P.; Strauss, S. H. *J. Am. Chem. Soc.* **1989**, *111*, 3762–3764.
- (52) Honeychuck, R. V.; Hersh, W. H. *J. Am. Chem. Soc.* **1989**, *111*, 6056–6070.
- (53) Colman, M. R.; Newbound, T. D.; Marshall, L. J.; Noirot, M. D.; Miller, M. M.; Wulfsberg, G. P.; Frye, J. S.; Anderson, O. P.; Strauss, S. H. *J. Am. Chem. Soc.* **1990**, *112*, 2349–2362.
- (54) Huhmann-Vincent, J.; Scott, B. L.; Kubas, G. J. *Inorg. Chem.* **1999**, *38*, 115–124.
- (55) Prestipino, C.; Regli, L.; Vitillo, J. G.; Bonino, F.; Damin, A.; Lamberti, C.; Zecchina, A.; Solari, P. L.; Kongshaug, K. O.; Bordiga, S. *Chem. Mater.* **2006**, *18*, 1337–1346.
- (56) Huheey, J. E.; Keiter, E. A.; Keiter, R. L. *Inorganic Chemistry: Principles of Structure and Reactivity*, 4th ed.; HarperCollins College: New York, 1993; p 404.
- (57) Chen, Z.; Xiang, S.; Zhao, D.; Chen, B. *Cryst. Growth Des.* **2009**, *9*, 5293–5296.
- (58) Tan, K.; Nijem, N.; Canepa, P.; Gong, Q.; Li, J.; Thonhauser, T.; Chabal, Y. J. *Chem. Mater.* **2012**, *24*, 3153–3167.
- (59) Okada, K.; Ricco, R.; Tokudome, Y.; Styles, M. J.; Hill, A. J.; Takahashi, M.; Falcaro, P. *Adv. Funct. Mater.* **2014**, *24*, 1969–1977.